Bulletin of the Seismological Society of America, Vol. 84, No. 3, pp. 806–816, June 1994

Slip Triggered on Southern California Faults by the 1992 Joshua Tree, Landers, and Big Bear Earthquakes

by Paul Bodin,[1] Roger Bilham, Jeff Behr, Joan Gomberg, and Kenneth W. Hudnut

Abstract Five out of six functioning creepmeters on southern California faults recorded slip triggered at the time of some or all of the three largest events of the 1992 Landers earthquake sequence. Digital creep data indicate that dextral slip was triggered within 1 min of each mainshock and that maximum slip velocities occurred 2 to 3 min later. The duration of triggered slip events ranged from a few hours to several weeks. We note that triggered slip occurs commonly on faults that exhibit fault creep. To account for the observation that slip can be triggered repeatedly on a fault, we propose that the amplitude of triggered slip may be proportional to the depth of slip in the creep event and to the available near-surface tectonic strain that would otherwise eventually be released as fault creep. We advance the notion that seismic surface waves, perhaps amplified by sediments, generate transient local conditions that favor the release of tectonic strain to varying depths. Synthetic strain seismograms are presented that suggest increased pore pressure during periods of fault-normal contraction may be responsible for triggered slip, since maximum dextral shear strain transients correspond to times of maximum fault-normal contraction.

Introduction

In this article we present and discuss observations from creepmeters of fault slip triggered remotely by the three largest earthquakes of the Landers earthquake sequence of April through June, 1992. Triggered fault slip is a form of aseismic fault creep which coincides closely in time with a large nearby earthquake, but is distinct from the primary rupture (Sylvester, 1986). Triggered fault slip of as much as 25 mm has been observed in southern California, although offsets are frequently less. The first unambiguous observations of the phenomenon followed the 1968 Borrego Mountain earthquake (Allen *et al.*, 1972). Subsequent examples included the 1979 Imperial Valley earthquake (Sieh, 1982; Fuis, 1982), the 1981 Westmoreland earthquake (Sharp *et al.*, 1986a), the North Palm Springs earthquake (Williams *et al.*, 1988; Sharp and *et al.*, 1986b), and the 1987 Superstition Hills earthquake (McGill and *et al.*, 1989; Hudnut and Clark, 1989). Triggered slip has also been observed from several recent central California earthquakes: the 1983 Coalinga earthquake (Mavko *et al.*, 1985; Schulz *et al.*, 1989), the 1984 Morgan Hill earthquake (Schulz, 1985), the 1986 Tres Pinos earthquake (Simpson *et al.*, 1988), and the 1989 Loma Prieta earthquake (Galehouse, 1990; McClellan and Hay, 1990).

Triggered slip is of interest for several reasons. First, there seem to be several seemingly inconsistent processes at work in the phenomenon that require reconciliation. A unified explanation for observations of triggered slip has yet to be forwarded. Second, triggered slip may hold clues about the rheological structure of the fault on which it is observed. Third, a slipping fault may act as a proxy for a strainmeter, permitting an assessment of shallow strains. Fourth, triggered fault slip may illuminate some of the processes operative in the widespread observations of remotely triggered seismicity subsequent to the Landers mainshock (e.g., Hill *et al.*, 1993).

Most examples of triggered slip in southern California have been field observations of surface cracks. Such observations offer little or no information on the timing of triggered slip development. Few earthquakes have triggered slip on faults in southern California monitored by creepmeters. McGill *et al.* (1989) studied records from creepmeters on the San Andreas and Imperial Valley faults at the time of the 1987 Superstition Hills earthquake sequence. At two surface sites, triggered slip took place within minutes of each of the two largest earthquakes of the sequence, which were separated in time by about 11 hr. At one site (Ross Road), a large slip event (~5 mm) commenced several hours after the second of the two largest earthquakes, with a duration

[1]Present address: Center for Earthquake Research and Information, Memphis State University, Memphis, Tennessee 38112.

of about 12 hr. From combined tiltmeter and creepmeter records, Williams *et al.* (1988) showed that slip on the San Andreas fault near the Salton Sea following the 1985 North Palm Springs earthquake probably initiated either at depth or elsewhere along the fault trace and then propagated into the section of the fault monitored by the creepmeter.

Prior to the Landers earthquake, triggered slip had been observed exclusively on faults known to be creeping aseismically. Complex perturbations in slip rates have been observed on creeping faults in central California for months and even years following moderate earthquakes (Burford and Harsh, 1980; Burford and Schulz, 1988). In this article we do not consider these long-term fluctuations, but restrict our attention to the first few days following a mainshock. The Landers sequence caused small amounts of slip on faults in the region that apparently did not have any major deep displacement, such as the Pisgah, Lenwood, Northwest Johnson Valley, and Calico faults. These faults were not known to have been creeping prior to the Landers sequence (Hart *et al.*, 1993). Bilham and Williams (1985) noted, and Williams *et al.* (1988) confirmed, that triggered slip on the southern San Andreas fault occurs only in regions oblique to the inferred slip vector where fault-normal contraction occurs. In adjoining segments of the fault not subject to this process, triggered slip has not been observed. The depths of triggered slip events are unknown but are assumed to be comparable to the depth of creep on faults where it is observed.

The causative mechanism of triggered slip is not known. Williams *et al.* (1988) concluded that a variety of factors were involved in determining where triggered slip took place and how much offset was observed. The amount of slip, although controlled in part by the amount of prestrain, seemed also to be affected by the presumed level of strong ground motion. Allen *et al.* (1972) concluded from observations following the 1968 Borrego Mountain earthquake that slip on the San Andreas fault was not driven by the "static" strains imposed by the remote fault rupture, because the change in the static strain field was of the wrong sign to cause the observed sense of triggered slip. They concluded that remote slip was dynamically triggered by the passage of transient seismic waves, and that it represented the release of shallow tectonic prestrain as a result of a slip deficit near the surface on creeping faults (see also Sharp *et al.*, 1986a, b). Because a very shallow slip deficit would suggest that the fault near the surface was stronger than at depth, which is counterintuitive, it seems more likely that the shallow part of the fault is simply weaker, and more susceptible to the triggering forces. Allen *et al.* (1972) also note that the manifestation of some triggered slip was apparently delayed. More recent studies, which have constrained the timing of triggered slip (Williams *et al.*, 1988; McGill *et al.*, 1989), demonstrate that while some examples of triggered slip appear to coincide with the passage of seismic waves from the mainshock, triggered slip may also develop slowly, or have delayed onset. In central California both triggered slip driven by the static strain changes and dynamically triggered slip have been hypothesized (e.g., Simpson *et al.*, 1988), the former at sites closer to the driving mainshock.

The seismotectonic significance of triggered slip is also unclear. Sieh (1982) suggested that a fault that manifests triggered slip may be in a preseismic phase, and hence likely to rupture seismically in the near future. He suggested that the Superstition Hills fault was likely to rupture after observing triggered slip from the 1979 Imperial Valley earthquake. Although this forecast for the Superstition Hills fault was fulfilled by the 1987 rupture there, McGill *et al.* (1989) and Hudnut and Clark (1989) pointed out that additional triggered slip took place after 1987, and concluded that triggered slip may take place at any time in the earthquake cycle. McGill *et al.* (1989) further concluded that triggered slip probably represents a characteristic style of shallow slip on certain faults. Hudnut and Clark (1989) also showed that a comprehensive list of triggered slip occurrences did not show the phenomenon to be at all reliable as a precursor. Seismic hazard studies (e.g., Wesnousky, 1986) have used the distribution of triggered slip along a fault to divide it into segments likely to rupture as a unit. Hudnut and Clark (1989) suggest, however, that both triggered slip and afterslip occur only where there is substantial thickness of sediments in southern California. They further show for the 1979 Imperial Valley and the 1968 Borrego Mountain earthquakes, at least, that triggered slip may be a form of long-term afterslip following earthquakes that occurred many years or decades earlier. They further conjecture that this may apply even many decades to centuries after a large earthquake.

The Landers Earthquake Sequence

The Landers earthquake sequence of 1992 began on 23 April, with the M_w 6.1 Joshua Tree earthquake (Fig. 1). This earthquake caused no primary surface rupture but the focal mechanism and aftershock pattern indicated rupture of a near-vertical N10°W striking fault (Sieh *et al.*, 1993). The M_w 7.3 Landers earthquake took place on 28 June, and was associated with about 70 km of almost purely dextral surface offsets of parts of the Camp Rock, Emerson, Homestead Valley, Johnson Valley, and Eureka Peak faults, as well as the previously unmapped Landers and Burnt Mountain faults (Sieh *et al.*, 1993). The M_w 6.2 Big Bear earthquake followed the Landers earthquake by about 3 hr. The focal mechanisms and aftershock distribution for this earthquake indicate left-lateral strike slip on a NE striking fault. Detailed seismological studies suggest that the Big Bear rupture was

temporally and spatially complex, involving several conjugate rupture planes (Jones and Hough, 1994).

Observations

At the time of the Landers earthquake sequence, six creepmeters were functioning on faults in southern California, five of which recorded triggered slip. Four of these were along the San Andreas fault, one on the Superstition Hills fault, and one on the San Jacinto fault (Figs. 1 and 2, Table 1).

The amplitudes of triggered slip recorded by the creepmeters are similar to measurements of offsets derived from examination of nearby surface fractures (Rymer, personal comm.). The creepmeter-derived slip amplitudes are generally somewhat greater than geologic measurements made at the same site, probably because the creepmeters extend several meters on either side of the fault and thus include distributed shear which is not manifest on cracks. Geologic observations of slip vary along the fault trace over tens of meters (Rymer, personal comm.), possibly as a result of the variable sampling of distributed shear. Triggered slip also varies along strike, so the total offset observed by a creepmeter at one site on the fault may not be the same as that observed at other points along the fault.

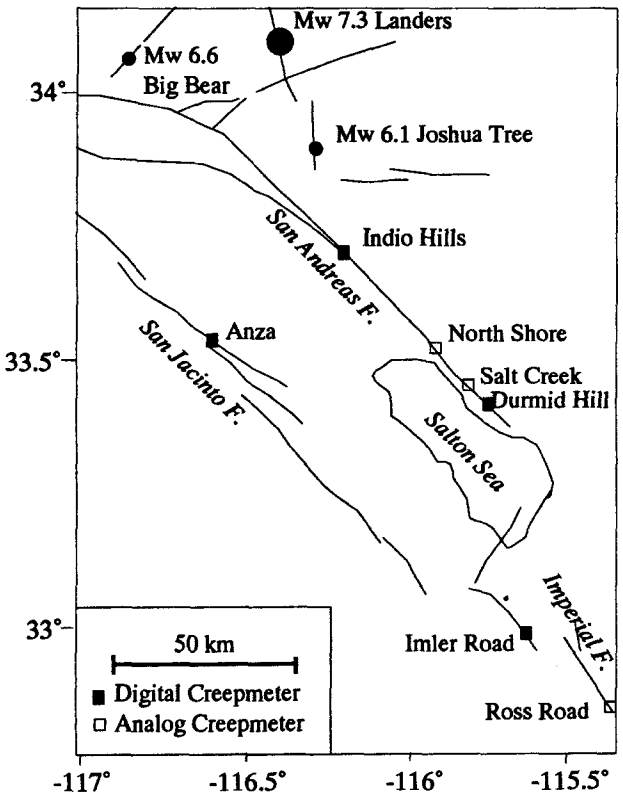

Figure 1. Location map. Epicenters of the three largest earthquakes of the 1992 Landers earthquake sequence are shown as circles. Digital creepmeter sites are shown as filled squares, analog creepmeter sites as open squares. Faults are represented by fine solid lines.

On the three digital creepmeters that recorded triggered slip, slip was initiated within 1 min after the origin time of the Landers earthquake (Fig. 3). At the two closest digital creepmeter sites which recorded triggered slip (Indio and Durmid), the peak slip velocity was attained within 2 min, while at the most remote site (Imler), it was attained within 3 min. The data are acquired once per minute within 1 sec of the start of each minute. Clocks in the computers were accurate to 1 sec, according to site visits 2 days after the event. We now summarize the observations at each creepmeter site.

Anza

This digital creepmeter did not register any signals at the time of the earthquakes of the Landers sequence. The instrument has measured no tectonic creep since its installation in January 1990, following a dramatic but short-lived increase in local seismicity, nor were ground cracks observed at this site when it was visited several weeks after the Landers mainshock.

Indio Hills

The digital instrument was installed in October 1989 and up to the time of the Landers events recorded a mean creep rate of less than 1 mm/yr. Prior to the Landers earthquake sequence, episodic creep (i.e., creep events) was absent at this site, and the offset was manifest as steady creep modulated by a seasonal signal, presumably related to thermoelastic effects. The Joshua Tree earthquake induced a creep event over 2 mm in amplitude, with a decay time constant on the order of a day. This was followed several days later by a much smaller creep event with a comparable decay rate (Fig. 4). The Landers earthquake subsequently triggered a creep event within a minute of the mainshock, which grew over a few days time to 4.1 mm. The Big Bear earthquake triggered no slip here. The fault was visited by geologists in the week following the Landers mainshock, who observed maximum displacements of ~10 mm on cracks within 10 m of the instrument (Rymer, personal comm.).

North Shore

Our analog observations from North Shore and Salt Creek include the time period of the Landers and Big Bear earthquakes only. As a result of thermoelastic and instrumental effects, the North Shore data are relatively noisy; however, dextral slip commenced soon after the Landers mainshock (Fig. 5). Because of the noise and the small amplitude of triggered slip, it is difficult to assess the true form of the creep event. It appears that slow, approximately linear slip occurs for about 12 hr, resulting in a total dextral slip of about 0.2 mm over the course of several days. Examination of the faults sub-

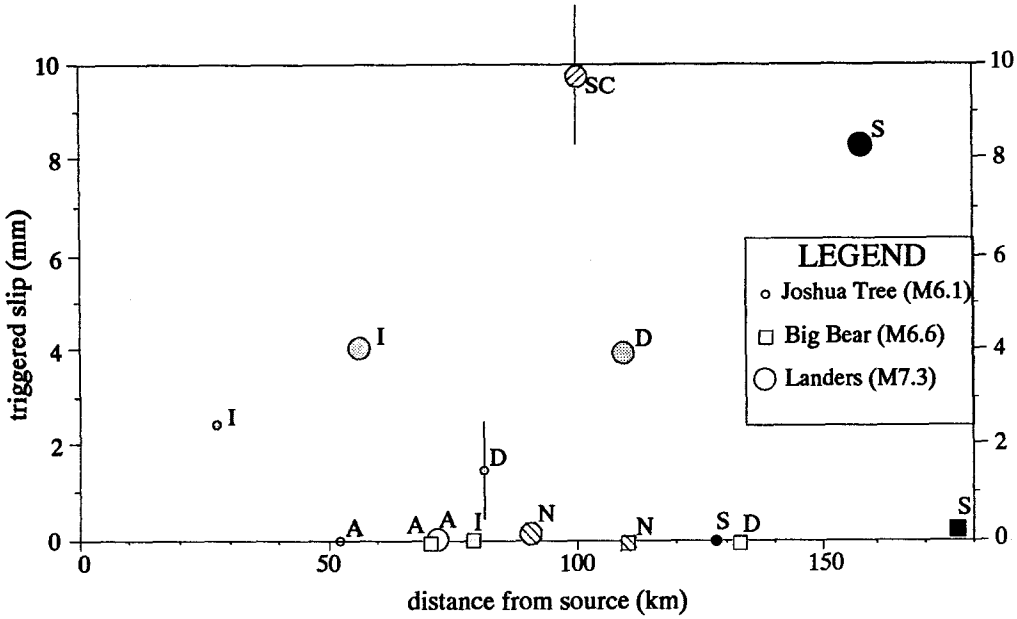

Figure 2. Triggered slip as a function of distance for the Joshua Tree, Landers, and Big Bear earthquakes. Different creepmeter sites are indicated by shading and by letters: I = Indio Hills (light shading), A = Anza (open symbols), D = Durmid Hill (dark shading), N = North Shore (hachures), SC = Salt Creek (hachures), and S = Superstition Hills (solid). Different earthquakes are shown by symbols of different sizes and shapes, as illustrated in legend. Vertical lines illustrate uncertainties associated with these observations.

Table 1

Distances and Amplitudes of Triggered Creep Events Observed at Southern California Creepmeters for the 1992 Landers Earthquake Sequence

Site **Operator** Fault	Latitude Longitude	Distance from Joshua Tree (km)	Amplitude (mm)	Distance from Landers (km)	Amplitude (mm)	Distance from Big Bear (km)	Amplitude (mm)
Anza	33.585°N						
CU Boulder	116.661°W	52.4	0	71.4	0	70.3	0
San Jacinto							
Durmid Hill	33.372°N						
CU Boulder	115.798°W	81.2	1.5 ± 1	109.3	3.9	132.6	0
San Andreas							
Indio Hills	33.740°N						
CU Boulder	116.184°W	27.5	2.4	56.2	4.1	78.5	0
San Andreas							
North Shore	33.250°N						
CalTech	115.941°W	93.5	?	117.4	~0.2	121.8	0
San Andreas							
Salt Creek	33.446°N						
CalTech	115.842°W	80.4	?	103.5	~10?	115.8	?
San Andreas							
Imler Road	32.927°N						
CU Boulder	115.701°W	128.2	0	156.9	8.2	176.0	0.2
Superstition Hills							

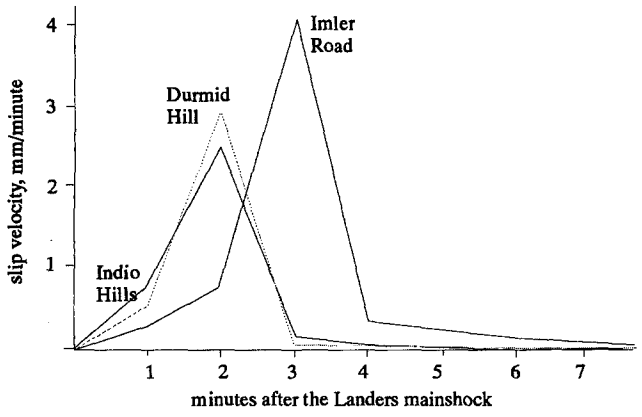

Figure 3. Triggered slip velocity on the southern San Andreas fault and the Superstition Hills fault at three digital creepmeter sites in the 7 min following the Landers mainshock. Samples are within 1 sec of the start of each minute.

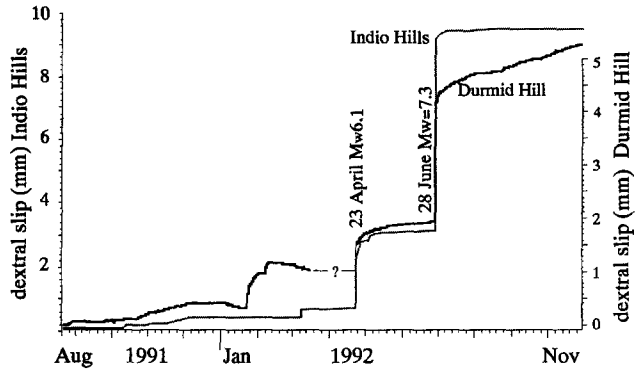

Figure 4. Creep between August 1991 and November 1992 on the southern San Andreas fault in the Indio Hills and at Durmid Hill. The Indio Hills record exhibits frictional effects (stiction) that makes the identification of events smaller than 200 μm uncertain. See text for a discussion of data.

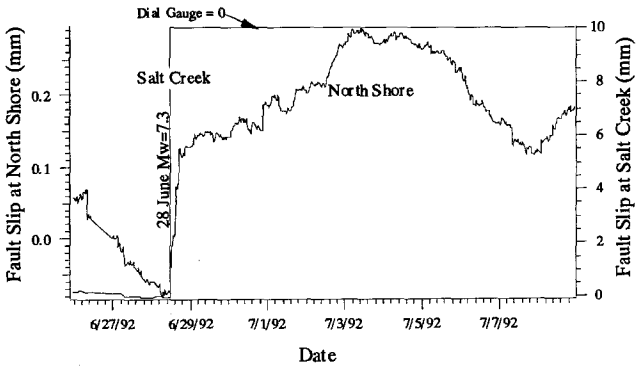

Figure 5. Creep between 26 June 1992 (day 178) and 8 July 1992 (day 190) on the southern San Andreas fault at the North Shore and Salt Creek creepmeters (Fig. 1).

sequent to the Landers rupture did not yield any observations of surface slip here (Rymer, personal comm.).

Salt Creek

The Salt Creek analog creepmeter apparently recorded a co-seismic offset from Landers greater than 9 mm (Fig. 5). However, the data are of questionable fidelity because, unlike the period immediately prior to the creep event, the signal from the creepmeter is unvarying immediately following the event, presumably as a result of friction associated with the zero-crossing point in the potentiometer sensor. Peak offsets of ~6 mm were observed at the surface next to the instrument (Rymer, personal comm.), which lends credence to the amplitude of the co-seismic offset.

Durmid Hill

The Durmid Hill digital creepmeter was installed in January 1990. During the year preceding the Joshua Tree earthquake, the creepmeter monitored a creep rate of approximately 1.5 mm/yr, comparable to the amplitude of thermoelastic signals in the data. However, subsequent to the Joshua Tree triggered slip episode and prior to the Landers mainshock, a continuous creep rate of ~2.1 mm/yr was established. After the Landers event, there was a further increase in the steady creep rate to about 4 mm/yr. The recording system malfunctioned in the weeks prior to the 23 April Joshua Tree earthquake, during a period of apparent left-lateral slip, and was restarted the day after the earthquake. When the instrument was restarted, the fault was evidently undergoing a vigorous, presumably triggered, slip event (Fig. 4). However, owing to the gap in the data, the precise amplitude of triggered offset from the Joshua Tree earthquake is uncertain. Based on the duration of the gap, the mean creep rate, and previous observations of the amount of apparent left-lateral slip during a rainy season, we estimate that the offset is somewhat greater than the ~0.5 mm observed after the instrument restarted, but not by more than 1 mm. For the Landers earthquake, triggered slip started within 1 min of the mainshock, and for the Joshua Tree earthquake, within 2 days. Each creep event lasts several days. Because of the steady creep following these events, however, it is difficult to assign an end to the triggered slip episodes. Slip was not triggered by the Big Bear event.

Imler Road

This digital creepmeter has operated on the Superstition Hills fault since the Superstition Hills earthquake in 1987. Prior to the earthquake in 1987, the fault was creeping at the rate of approximately 0.5 mm/yr, and since the earthquake there has been continuing decaying afterslip (Bilham, 1989). In the year prior to the Landers sequence the average creep rate was approximately 15 mm/yr. The afterslip at the site consists of both steady

creep and episodic creep, which Bilham and Behr (1992) interpreted as being a result of a two-layered fault rheology. The creep during the 2 yr prior to Landers has been contained in a relatively narrow range (shaded region in Fig. 6), in which afterslip obeys an approximate power-law decay in rate, and slip events occur in partly slip-predictable and partly time-predictable sense. That is, surface creep is currently occurring at a mean rate of 15 mm/year, and slip occurs always before approximately 14 mm of slip is overdue (the lower bound of the shaded region in Fig. 6). When slip occurs, the amplitude of the creep event never exceeds that needed to completely release accumulated slip (the upper bound of the shaded region in Fig. 6 may be considered to be a completely relieved state). The Joshua Tree earthquake triggered no slip. On 11 May 1992 a natural (not triggered) creep episode partially released surface strain when the surface slip reached its extreme maximum overdue level of ~14 mm. Approximately 6 weeks later the Landers earthquake triggered a creep event that brought the fault closer to its "completely relieved" level, which was supplemented by a 0.2-mm increment at the time of the Big Bear earthquake. Surface observations after the Big Bear earthquake showed a maximum offset of 20 mm on the Superstition Hills fault (at some distance from the digital creepmeter site; Rymer, personal comm.).

Dynamic Strains and Triggered Slip Mechanisms

The observations we have presented demonstrate that slip triggered remotely on southern California faults by earthquakes of the Landers sequence was initiated during or very soon after the passage of seismic waves. The location and amount of triggered slip are presumably related to some characteristic of the strain transients associated with surface waves, which are the most energetic seismic waves at regional distances. At the same time, triggered slip presumably also requires a capable fault ripe for triggering. We have investigated the potential of dynamic strains associated with propagating surface waves to remotely trigger surface slip.

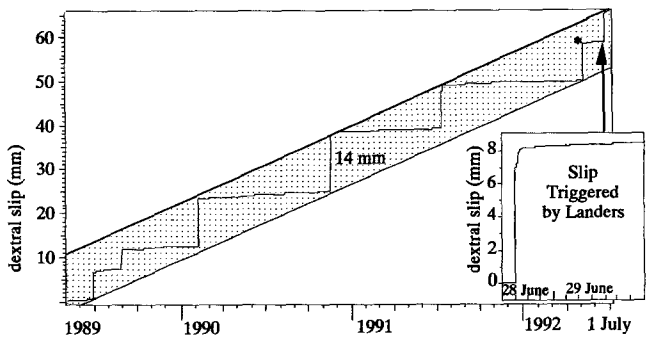

Figure 6. Creep and triggered slip on the Superstition Hills fault near Imler Road. At this site, creep events always occur between two well-established limits with similar slopes and a separation of ≈14 mm (shaded region). The upper limit is presumed to correspond to a condition of strain relief and the lower limit to one of maximum stored elastic strain. Triggered slip brought the slip condition close to complete strain release following a moderate natural creep event (indicated by an asterisk) 6 weeks earlier.

We used a synthetic strain seismogram technique to calculate the dynamic strains associated with the surface waves at creepmeter sites. The methods were developed and described in detail by Gomberg and Bodin (1994). Strain seismograms are calculated assuming a locked-mode, traveling-wave representation of the seismic wave field, containing the fundamental mode and five higher-mode Love and Rayleigh waves. The velocity structure for the Landers and Joshua Tree earthquakes and the source model for the Landers earthquake are identical to those used by Gomberg and Bodin (1994) to model seismograms for southern Nevada. The source model for Joshua Tree is a point source of scalar seismic moment 1.7×10^{25} dyne-cm located 12-km deep at 33.961°N, 116.318°W and corresponding to slip on a vertical dextral fault striking N10°W (Sieh *et al.*, 1993). The source spectrum was modified to account for source finiteness, assuming unilateral northward propagation at 3 km/sec from the epicenter on a 10-km-long fault. The method leads to the complete dynamic strain tensor, which we then resolve into components of physical significance with respect to the fault at the site of triggered slip. Those components are (1) the strike-slip shear strain, (2) the normal strain perpendicular to the fault plane, and (3) the volumetric strain.

We are unaware of seismic data available from sites collocated with creepmeters and thus are unable to test our model assumptions rigorously. There are several theoretical limitations of the synthetic model results. The method assumes that the source-receiver distance is greater than a few wavelengths: for waves with a period of 10 sec and a phase velocity of 3 km/sec three wavelengths would be 90 km. Furthermore, the method used to include the effect of source finiteness on strain is not applicable at distances less than about 2 source radii (at the frequency band of interest). Therefore, we restrict our analysis to the farthest creepmeter sites at Imler Road and Durmid Hill (Table 1) and interpret the results qualitatively.

Coulomb Failure

In Figure 7 we present synthetic strain seismograms for the Joshua Tree and Landers earthquakes at the sites of the Durmid Hill and Imler Road creepmeters. For each case we plot the normal strains perpendicular to the fault with the strike-slip shear strains (*top*) and the fault-normal strains with the volumetric strain (*bottom*). The

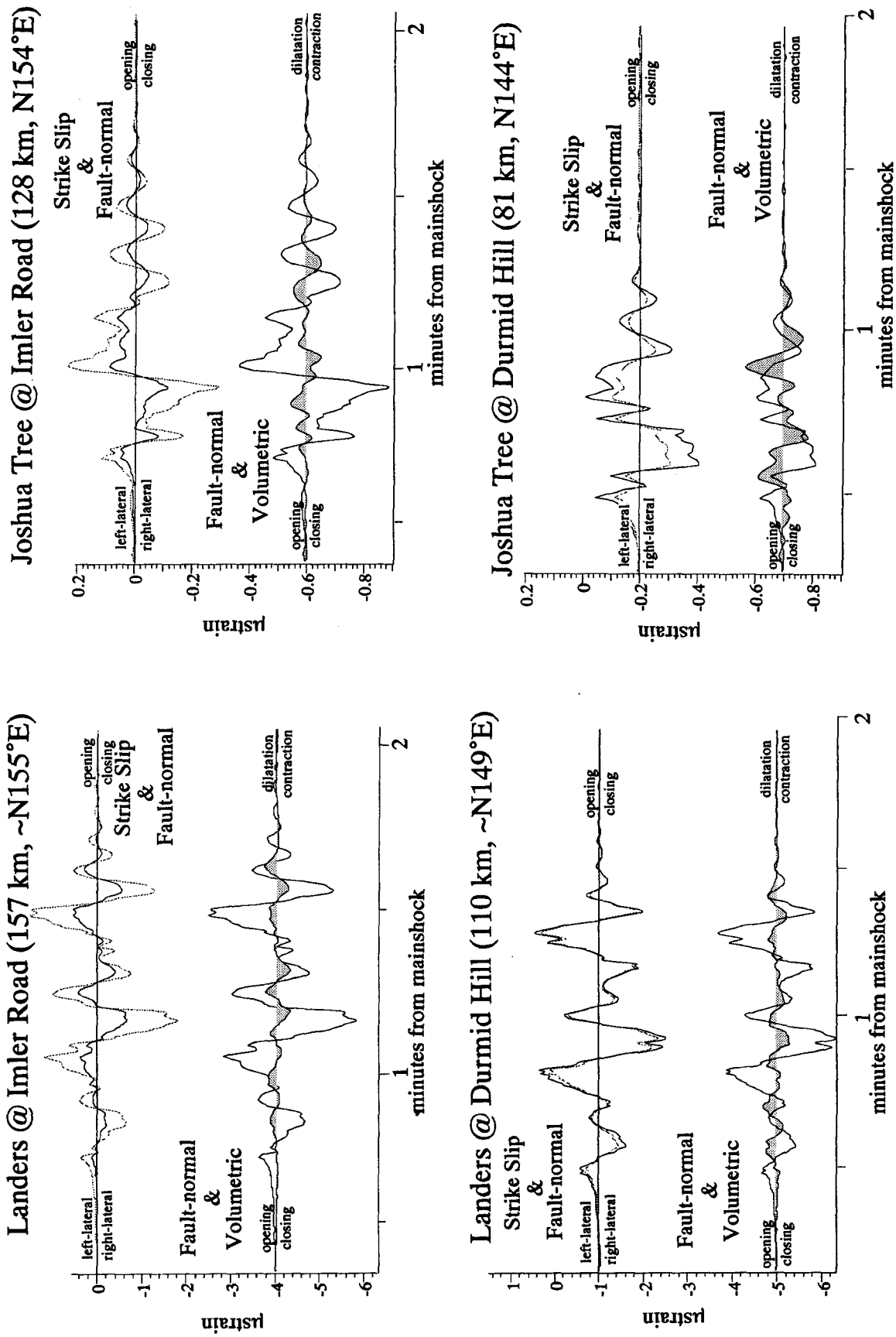

Figure 7. Synthetic strain seismograms at Imler Road and Durmid Hill for the Joshua Tree and Landers earthquakes. See text for a discussion of the methods used. The two left panels are strain seismograms from the Landers earthquakes at the two sites, while the two right-hand panels are from the Joshua Tree earthquake. The dynamic strain tensor has been resolved onto the local fault plane at each creepmeter site. Each panel consists of an upper and lower set of strain seismograms. The top set of seismograms superimposes the strike-slip (solid) and fault-normal (dashed) strain transients. The bottom set superimposes the fault-normal (solid), and the volumetric (shaded to zero) strain components.

dip-slip shear strains are zero at the free surface. We interpret the top plot in terms of its effects on a fault controlled by Coulomb failure for a dry medium, assuming that the relevant components of dynamic stresses are in phase with, and proportional to, the corresponding dynamic strain components. For an isotropic elastic material this assumption is well met when volumetric strains are either of the same sign as the fault-normal strains or smaller by a factor of about 2. In Figure 7, these conditions are generally valid, except for very brief periods in the strain seismogram of the Joshua Tree earthquake at Durmid Hill. If the frictional stress is proportional to the normal stress, then opening strains would tend to release the fault, allowing it to slip in the direction of the shear strain applied at that moment. The in-phase relationship between the strike-slip and fault-normal dynamic shear strain components for all four cases in Figure 7 illustrate that when the fault-normal strains are "releasing," the dynamic strain transient is driving the fault left-laterally. Because all observed offsets are dextral, it is clear that only a negative friction coefficient could lead to the observations. We conclude that the dynamic strain transient for both the Landers and Joshua Tree earthquakes could not induce the observed slip at the surface on a fault governed by Coulomb failure. Preexisting dextral, simple shear strain parallel to the fault (presumably the result of tectonic processes) would add dextral shear to the strike-slip strain seismograms, which would have the effect of subtracting a DC offset (Fig. 7). If the offset was large enough, when the fault-normal strains were in the opening sense and the total strike-slip strain was dextral (despite the sinestral sense of the transient at that moment), then the transient might aid slip. This failure mechanism is more plausible for the Joshua Tree earthquake, because the transient strains were about a factor of 10 smaller than for the Landers earthquake, thereby requiring much smaller preexisting dextral strains to permit dextral slip.

Modified Coulomb Failure Conditions

We also consider the possibility that a simple Coulomb failure condition is not the appropriate failure condition on the fault to cause triggered slip. In particular, it is plausible to invoke a fault zone consisting of fluid-filled voids that become overpressured during a suitable combination of transient shear stress and fault-normal stress (Blanpied *et al.*, 1992). The in-phase correspondence between synthetic fault-normal contraction and dextral shear in Figure 7 would suggest that such a mechanism for triggered slip may be quite likely. Moreover, the restriction of triggered slip to transpressive segments of the southern San Andreas is consistent with an overpressuring mechanism, for it is in those regions where high ambient pore pressures are most likely to prevail. On Durmid Hill, in the Mecca Hills, and in the Indio Hills numerous seeps occur along the fault zone. Along these zones, the soil is moist even during the hottest and driest weather conditions. These seeps are long-lived features, as evidenced by the growth of large clumps of shrubs. Apparently, these seeps are continuously active, suggesting upward fluid flow within the fault zones. Natural seeps also occur along the San Andreas fault to the northwest, particularly in the vicinity of the Mecca Hills and Indio Hills, for instance, northwest of Thousand Palms Canyon on the Banning strand.

In addition to modeling uncertainties, which may modify the precise phase relationships of dynamic strains and their relative magnitudes, dynamic amplification in the sediments of the Imperial and Coachella Valleys may modify, in significant ways, the phase relationship of fault-normal and fault-parallel strain fields. Seismic wave studies reveal that amplitudes in the center of Coachella Valley are more than an order of magnitude larger than on its margins (Field *et al.*, 1992). Further amplification of applied strains in the fault zone are possible if parts of the fault act as a weak inclusion with greater compliance than the surrounding materials (King *et al.*, 1977). Even without fault zone amplification, strains with magnitudes approaching 10 microstrain or greater are theoretically possible under certain circumstances.

Depth-Dependent Strain Release

One of the enigmatic features of triggered slip is that the same fault segment may slip again after a second earthquake occurring within hours or days of the first. If the slip is driven by local strains, these must be incompletely released by the first earthquake of the sequence. Observations of triggered slip cannot be reconciled with a simple slip-predictable process. If triggered slip were slip-predictable, the amount of slip triggered would be simply related to the time since the last triggered event, driven presumably by regional shear strain increase related to plate motion (e.g., at <0.5 μstrain/yr in the Coachella Valley; Lisowski *et al.*, 1991). An example of data incompatible with a slip-predictable process are the 1987 data from Salt Creek (McGill *et al.*, 1989) when slip on the southern San Andreas fault was triggered by the Elmore Ranch (1.3 mm) and Superstition Hills (1.7 mm) earthquakes, 11 h apart. Triggered slip is evidently responsive to some characteristic of the wave train that triggers slip. We propose that dynamic strain transients from surface waves originating from successive earthquakes may each trigger complete strain-drops, but lead to slip at different depths on a remote fault. If subsequent seismic strain transients induce slip at progressively greater depth on the creeping fault, additional triggered slip can occur. The weak relation in Figure 2 between increased triggered slip amplitude and distance for the Landers earthquake inversely mimics a decrease of slip with distance from the Joshua Tree

earthquake, and may be a manifestation of this effect. The larger longer-period surface waves from the Landers earthquake presumably liberate strain stored deeper and farther from the triggered fault, up to such distances that the surface wave amplitudes are sufficiently attenuated. The general lack of triggered slip following the Big Bear earthquake (except for a very small step at Imler Road), which was larger than the Joshua Tree earthquake, is consistent with this interpretation.

Allen *et al.* (1972) observed that the small amplitude of surface slip (≈1 cm) and its relatively large along-strike distribution (>70 km on occasion) requires triggered slip to be a surface phenomenon. Were it to penetrate to seismogenic depths, it would presumably obey a scaling law typical of fault rupture, demanding two orders of magnitude greater slip for comparable rupture lengths. Yet, although the depth of slip must be shallow, perhaps limited to the <3-km depths of sediments along much of the Coachella Valley cut by creeping faults, we have no direct measure of the depth of this slip. Since the depth to which creep occurs determines the surface creep rate of a creeping fault (e.g., Bilham and Behr, 1992), it follows that the magnitude of triggered slip is proportional to the depth to which it occurs. If we suppose that this depth is not constant but is a function of the amplitude and wavelength of propagating surface waves traversing the fault, it is possible to modify a slip-predictable model to permit repeated triggering on a fault to sequentially greater depths. A fault that is triggered by one wave train may be triggered again by another, as long as that second wave train is able to induce fault slip to greater depth. A fault that is triggered by one wave train may be triggered again by another, as long as the second wave train is able to induce fault slip to greater depth. We propose that if the second wave train is unable to increase the depth of slip, it is unable to "access" additional strain energy and no additional triggering will occur.

The relation between the surface fault offset, Δu, and the depth of creep is:

$$\Delta u = 2\frac{\epsilon H}{\pi}\cosh^{-1}\left(\frac{3-\cos(\pi b/H)}{1+\cos(\pi b/H)}\right),$$

(Tse *et al.*, 1986) which is approximately linear when the depth of creep, b, is much less than the thickness of the elastic plate, H, and where ϵ is the imposed shear strain. Thus, for the 1987 Salt Creek data, we would infer that the depth of surface slip increased by a factor of 1.3 between the Elmore Ranch and Superstition mainshocks, as a result of the larger-amplitude surface waves generated by the larger second event, and the consequently larger surface waves traversing the San Andreas fault from this event. As in Bilham and Behr (1992), who were unable to infer the absolute depth of creep of episodic and shallow background processes, we are unable to infer the depth of triggered slip in each event, but are able to estimate the ratio of the two depths that may have been active.

Discussion

There is evidently no simple relation between the amplitude of triggered slip and its distance from a causal earthquake. It is possible from some of our data to conclude that the amplitude of slip remotely triggered by the Landers earthquake increased with distance from the causal rupture (Fig. 2), suggesting that alone, the intensity of shaking is insufficient to moderate triggered slip amplitude. Creepmeter observations indicate that the triggered slip is initiated close to the time of arrival of seismic waves propagating from large nearby earthquakes. We find, however, that the available data permit several different physical mechanisms. We suggest that a strain-monitoring array with a bandwidth from DC to about 1 Hz is necessary to resolve the causative mechanism of triggered slip. Such a network would be able to determine the depth to which strain on the fault was relieved and the amplitude and orientations of the causative strain transients. Moreover, such a test is considerably simplified in southern California, because triggered slip has now been observed on more than five occasions on some fault segments. It is clear on which fault segments triggered slip is to be expected.

Conclusions

The absence of strain measurements or strong motion seismometers near creepmeters on triggered faults hinders a precise quantitative analysis of the wave combination responsible for triggered slip. Synthetic surface wave strain seismograms suggest, however, that the most likely combination may occur during fault-normal contraction of the fault in conjunction with increased dextral shear strain. The transient conditions we calculate to have prevailed on triggered faults in the Landers sequence suggest that a simple Coulomb failure condition cannot be responsible for the observed dextral slip, because times of maximum fault-releasing fault-normal strains correspond to times of induced sinestral shear. Thus, we propose that transient increased pore pressures occur during fault-normal contraction, thereby reducing the effective normal stress across the fault at the moment that transient shear strains increase dextral shear. We further propose that triggered slip represents the release of slip on a remote, usually creeping, fault within several minutes of a mainshock, to a depth that is proportional to the amplitude and depth of transient strains applied to the fault by propagating seismic waves. Observations from past triggered events only hours apart suggest that both the amplitude and wavelength of transient strain fields

are of importance in triggering the release of near-fault strain energy. A second triggered event may occur if the fault is caused to slip at increasingly greater depth.

Triggered slip is reported commonly from creeping faults in southern California that pass through sediment-filled valleys. The amplitude of transient strains in the sediments of the Imperial and Coachella Valleys may be significantly enhanced relative to bedrock strain amplitudes, resulting in the amplification of transient strains associated with surface waves. Thus, the frequent triggering of faults in southern California by nearby earthquakes may be favored by their location in sedimentary basins.

Acknowledgments

The digital creepmeters are maintained by USGS grant 14-08-001-G1876, and the Caltech analog creepmeters by USGS 14-08-0001-G1666 and USGS 14-08-0001-G1990. This work was supported in part by USGS 1434-93-G-2356. We thank Kerry Sieh, Clarence Allen, David Johnson, and Wayne Miller for data from the Caltech creepmeters.

References

Allen, C. R., M. Wyss, J. N. Brune, A. Granz, and R. Wallace (1972). Displacements on the Imperial, Superstition Hills, and San Andreas faults triggered by the Borrego Mountain Earthquake, in *The Borrego Mountain Earthquake, U.S. Geol. Surv. Profess. Pap.* **787**, 87–104.

Bilham, R. and P. Williams (1985). Sawtooth segmentation and deformation processes on the southern San Andreas fault, California, *Geophys. Res. Lett.* **12**, 557–560.

Bilham, R. (1989). Surface slip subsequent to the 24 November 1987 Superstition Hills, California, earthquake monitored by digital creepmeters, *Bull. Seism. Soc. Am.* **79**, 424–450.

Bilham, R. and J. Behr (1992). A two-layer model for aseismic slip on the Superstition Hills fault, California, *Bull. Seism. Soc. Am.* **82**, 1223–1235.

Blanpied, M. L., D. A. Lockner, and F. D. Byerlee (1992). An earthquake mechanism based on rapid sealing of faults, *Nature* **358**, 574–576.

Burford, R. O. and P. W. Harsh (1980). Slip on the San Andreas fault in central California from alignment array surveys, *Bull. Seism. Soc. Am.* **70**, 1322–1351.

Burford, R. O. and S. S. Schulz (1988). A current retardation rate of aseismic slip on the San Andreas fault at San Juan Bautista, *EOS* **69**, 1424.

Field, E. H., K. H. Jacob, N. Barstow, and P. Friberg (1992). Preliminary results from a site response study conducted in the Coachella Valley following the Landers and Big Bear earthquakes, *EOS* **73**, 383.

Fuis, G. S. (1982). Displacement on the Superstition Hills fault triggered by the earthquake, in *The Imperial Valley Earthquake of October 15, 1979, U.S. Geol. Surv. Profess. Pap.* **1254**, 145–154.

Galehouse, J. S. (1990). Effect of the Loma Prieta earthquake on surface slip along the Calveras fault in the Hollister area, *Geophys. Res. Lett.* **17**, 2019–2022.

Gomberg, J. S. and P. Bodin (1994). Triggering of the M_s = 5.4 Little Skull Mountain, Nevada Earthquake with Dynamic Strains *Bull. Seism. Soc. Am.* **84**, no. 3, 844–853.

Hill, D. P., P. A. Reasenberg, A. Michael, W. J. Arabaz, G. Beroza, D. Brumbaugh, J. N. Brune, R. Catro, S. Davis, D. dePolo, W. L. Ellsworth, J. Gomberg, S. Harmsen, L. House, S. M. Jackson, M. J. S. Johnston, L. Jones, R. Keller, S. Malone, L. Munguia, S. Nava, J. C. Pechmann, A. Sanford, R. W. Simpson, R. B. Smith, M. Stark, M. Stickney, A. Vidal, S. Walter, V. Wong, and J. Zollweg (1993). Seismicity remotely triggered by the magnitude 7.3 Landers, California, earthquake, *Science* **260**, 1617–1623.

Hart, E. W., W. A. Bryant, and J. A. Treiman (1993). Surface faulting associated with the June 1993 Landers earthquake, California, *Calif. Geology* **16**, 10–16.

Hudnut, K. W. and M. M. Clark (1989). New slip along parts of the 1968 Coyote Creek fault rupture, California, *Bull. Seism. Soc. Am.* **79**, 451–465.

Jones, L. E. and S. E. Hough (1994). Analysis of broadband records from the June 28, 1992 Big Bear earthquake: Evidence of a multiple-source event. *Bull. Seism. Soc. Am.* (in press).

King, C., R. D. Nason, and R. O. Burford (1977). Coseismic steps recorded on creepmeters along the San Andreas fault, *J. Geophys. Res.* **82**, 1655–1662.

Lisowski, M., J. C. Savage, and W. H. Prescott (1991). The velocity field in central California, *J. Geophys. Res.* **96**, 8369–8389.

Mavko, G. M., S. Schulz, and B. D. Brown (1985). Effects of the 1983 Coalinga, California earthquake on creep along the San Andreas fault, *Bull. Seism. Soc. Am.* **75**, 475.

McClellan, P. H. and E. A. Hay (1990). Triggered slip on the Calaveras fault during the Magnitude 7.1 Loma Prieta earthquake, *Geophys. Res. Lett.* **17**, 2027–2030.

McGill, S. F., C. R. Allen, K. W. Hudnut, D. C. Johnson, W. F. Miller, and K. E. Sieh (1989). Slip on the Superstition Hills fault and on nearby faults associated with the 24 November 1987 Elmore Ranch and Superstition Hills Earthquakes, southern California, *Bull. Seism. Soc. Am.* **79**, 362–375.

Schulz, S. S. (1985). Triggered creep near Hollister after the April 24, 1984, Morgan Hill, California earthquake, in *The 1984 Morgan Hill, California Earthquake*, J. H. Bennet and R. W. Sherburne (Editors), *Calif. Div. Mines Geol. Spec. Pub.* **687**, 175–182.

Schulz, S. S., G. M. Mavko, and B. D. Brown (1989). Response of creepmeters on the San Andreas fault near Parkfield to the Earthquake, in *The Coalinga, California, Earthquake of May 2, 1983, U.S. Geol. Surv. Profess. Pap.* **1487**, 409–417.

Sharp, R. V., M. J. Rymer, and J. J. Lienkaemper (1986a). Surface displacements on the Imperial and Superstition Hills faults triggered by the Westmorland, California, earthquake of 26 April 1981, *Bull. Seism. Soc. Am.* **76**, 949–965.

Sharp, R. V., M. J. Rymer, and D. M. Morton (1986b). Trace-fractures on the Banning fault created in association with the 1986 North Palm Springs earthquake, *Bull. Seism. Soc. Am.* **76**, 1838–1843.

Sharp, R. V., M. J. Rymer, and D. M. Morton (1986b). Trace-fractures on the Banning fault created in association with the 1986 North Palm Springs earthquake, *Bull. Seism. Soc. Am.* **76**, 1838–1843.

Sieh, K. E. (1982). Slip along the San Andreas associated with the earthquake, in *The Imperial Valley Earthquake of October 15, 1979, U.S. Geol. Surv. Profess. Pap.* **1254**, 155–160.

Sieh, K., L. Jones, E. Hauksson, K. Hudnut, D. Eberhart-Phillips, T. Heaton, S. Hough, K. Hutton, H. Kanamori, A. Lilje, S. Lindvall, S. F. McGill, J. Mori, C. Rubin, J. A. Spotila, J. Stock, H. K. Thio, J. Treiman, B. Wernicke, and J. Zachariasen

(1993). Near-field investigations of the Landers earthquake sequence, April to July 1992, *Science* **260**, 171–176.

Simpson, R. W., S. S. Schulz, L. D. Dietz, and R. O. Burford (1988). The response of creeping parts of the San Andreas fault to earthquakes on nearby faults: two examples, *Pageoph* **126**, 665.

Sylvester, A. G. (1986). Near-field tectonic geodesy, in *Active Tectonics (Studies in Geophysics Series)*, National Academy Press, Washington, D. C., 164–180.

Tse, S. T. and J. R. Rice (1986). Crustal earthquake instability in relation ot the depth variation of frictional slip properties, *J. Geophys. Res.* **91**, 9452–9472.

Wesnousky, S. G. (1986). Earthquakes, quaternary faults, and seismic hazard in California, *J. Geophys. Res.* **91**, 12587–12631.

Williams, P. L., S. F. McGill, K. E. Sieh, C. R. Allen, and J. N. Louie (1988). Triggered slip along the San Andreas fault after the 8 July 1986 North Palm Springs earthquake, *Bull. Seism. Soc. Am.* **78**, 1112–1122.

CIRES
University of Colorado
Boulder, CO 80309
(P.B., R.B., J.B.)

U.S. Geological Survey
Denver Federal Center
Denver, CO 80225
(J.G.)

U.S. Geological Survey
Pasadena, CA 91106
(K.W.H.)

Manuscript received 2 August 1993.